REPORT DOCUMENTATION PAGE

Form Approved
OMB No. 0704-0188

1. REPORT DATE *(DD-MM-YYYY)*	**2. REPORT TYPE**	**3. DATES COVERED** *(From – To)*
15-09-2021	Final Report	06-08-2018 to 15-09 2021

4. TITLE AND SUBTITLE

Manipulation of Neuronal Excitation Using Fast Thermal Gradient

5a. CONTRACT NUMBER

5b. GRANT NUMBER
N/A

5c. PROGRAM ELEMENT NUMBER
61102F

6. AUTHOR(S)

Christopher Valdez (Ibtissam Echchgadda)

5d. PROJECT NUMBER

5e. TASK NUMBER

5f. WORK UNIT NUMBER
H10P

7. PERFORMING ORGANIZATION NAME(S) AND ADDRESS(ES)
Air Force Materiel Command, Air Force Research Laboratory, 711th Human Performance Wing, Human Effectiveness Directorate, Bioeffects Division, Radio Frequency Bioeffects Branch (711 HPW/RHDR)
4141 Petroleum Road
JBSA Fort Sam Houston, Texas 78234-2644

8. PERFORMING ORGANIZATION REPORT NUMBER

LRIR 18RHCOR039

9. SPONSORING / MONITORING AGENCY NAME(S) AND ADDRESS(ES)
Air Force Materiel Command, Air Force Research Laboratory, 711th Human Performance Wing, Human Effectiveness Directorate, Bioeffects Division, Radio Frequency Bioeffects Branch (711 HPW/RHDR)
4141 Petroleum Road
JBSA Fort Sam Houston, Texas 78234-2644

10. SPONSOR/MONITOR'S ACRONYM(S)
711 HPW/RHDR

11. SPONSOR/MONITOR'S REPORT NUMBER(S)

AFRL-RH-FS-SR-2021-0001

12. DISTRIBUTION / AVAILABILITY STATEMENT
DISTRIBUTION A: Approved for public release, distribution unlimited. PA # TSRL-PA-2020-0199, Oct 2020.

13. SUPPLEMENTARY NOTES

14. ABSTRACT

This report summarizes the work completed during our LRIR tenure. The overarching goal of this project was to explore the fundamental biophysical interactions of infrared (IR)-induced fast thermal gradients (FTG) within biological systems. Throughout this effort, we focused on developing *in silico* models that are representative of the energy delivered by the IR exposure. As a result, we have developed a model that is spatially and temporally representative of the IR exposure on the cell surface. In addition, we have added critical details that contribute to an *in vitro* experimental platform for IR applications.

15. SUBJECT TERMS
Infrared, induced fast thermal gradients, in silico models, IR application

16. SECURITY CLASSIFICATION OF:			**17. LIMITATION OF ABSTRACT**	**18. NUMBER OF PAGES**	**19a. NAME OF RESPONSIBLE PERSON**
a. REPORT	**b. ABSTRACT**	**c. THIS PAGE**			C. Valdez/ I. Echchgadda
Unclassified	Unclassified	Unclassified	SAR	18	**19b. TELEPHONE NUMBER** (include area code) N/A

FINAL LABORATORY TASK REPORT

LRIR #: 18RHCOR039

Title: Manipulation of Neuronal Excitation Using Fast Thermal Gradient

Reporting Period: FY20

Laboratory Task Manager: Dr. Christopher Valdez, 711 HPW/RHDR

Commercial Phone: 210-539-8199 **DSN:** 389-8199 **FAX:** 210-539-7285

Mailing Address: 4141 Petroleum Road, JBSA Fort Sam Houston, TX 78234-2644

E-Mail Address: christopher.valdez.5@us.af.mil

AFOSR Program Manager: Dr. Sofi Bin-Salamon

Research Objectives:

This report summarizes the work completed during our LRIR tenure. The overarching goal of this project was to explore the fundamental biophysical interactions of infrared (IR)-induced fast thermal gradients (FTG) within biological systems. Throughout this effort, we focused on developing *in silico* models that are representative of the energy delivered by the IR exposure. As a result, we have developed a model that is spatially and temporally representative of the IR exposure on the cell surface. In addition, we have added critical details that contribute to an *in vitro* experimental platform for IR applications. Overall, the development of our IR modeling capabilities, and an *in vitro* experimental platform has provided the scientific foundation for us to investigate the biophysical mechanisms that underlie the cellular response to IR exposures. In particular, we focused on how an IR exposure can modulate the plasma membrane, and calcium dynamics within the cell (Aim 1-2). In addition, in Aim 3, we highlight our most recent efforts to determine IR-specific calcium channel modulation, and how fine-tuning of IR inputs can uniquely modify biophysical mechanisms within the cell.

Specific Aims

1. Determine the effect of IR-induced exposure on the plasma membrane
2. Define how calcium dynamics are modified by an IR exposure
3. Identify calcium channels modified by IR exposure, and make advancements towards physiologically relevant IR input parameters

Technical Summary:

Brief Description of Technical Approach

As an infrared pulse (IRP) travels through biological media (predominantly water) it is absorbed, causing a temporal and spatial thermal gradient that can interact with cells. We hypothesize that thermal gradient plays a role in modifying electrical signals within cells. In order to test our hypothesis, we first generated a computational simulation of the IR pulse within an *in vitro* experimental platform. Furthermore, we aimed to link our IR modeling efforts with numerical simulations that represent membrane charging across the plasma membrane. To this end, we utilized the Scalable Effects Simulation Environment (SESE). This approach can very accurately compute the dosimetry of laser energy deposited in a physical neuron structure and calculate the resultant transient thermal diffusion. However, SESE was not designed to model the neural action potential impact from the resultant thermal gradient. To model this portion of the problem, the time-temperature history data from SESE needed to be coupled to a model that could calculate the membrane potential and resultant inhibition or stimulation effect. For this modeling, we collaborated with researchers at Vanderbilt University who had been working with a model produced at Yale called NEURON. This model accepts axonal membrane properties including physiological conditions and generates a set of ordinary differential equations representing the circuit equivalent of ion channel behavior (which can be modified). It then solves this set of equations and predicts nerve behavior under the provided conditions. In collaboration with Vanderbilt, we used this capability to test a temperature dependent Hodgkin-Huxley model for neuron behavior. Figure 1 shows the end-to-end coupling between the SESE and NEURON model.

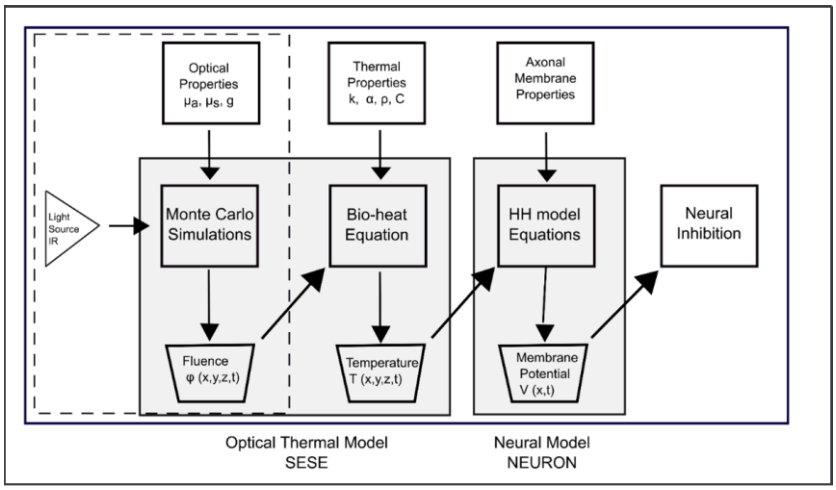

Figure 1: Data flow diagram showing the laser propagation and heat solving code coupled to a neural membrane potential model.

Coupling the models into a single tool presented two major challenges: 1) SESE requires high performance computing hardware to accelerate computations, and 2) there is not a single "interface" that can control both the SESE and NEURON models. To overcome these challenges, a tool called Dakota (open source software developed by Sandia) was utilized to wrap the two models into a set of execution steps with preprocessing and post processing steps to transmit data between the models. Once the models were joined, a gradient-based optimization algorithm was employed to search for conditions required to produce threshold level effects.

To test the coupled model, a prototype geometry similar to lab conditions at Vanderbilt were used as an initial test case. Figure 2 shows the laser fiber represented by a vertical red cylinder placed perpendicular to a neuron represented by a horizontal blue cylinder half embedded in dermis tissue. A stimulus is provided as an initial condition on one end of the neuron and is propagated to the other end. This propagation is blocked if laser heating causes the maximum membrane voltage along the nerve to drop below a set threshold. Figure 3 shows a simulated action potential block produced as a result of a laser-induced thermal gradient.

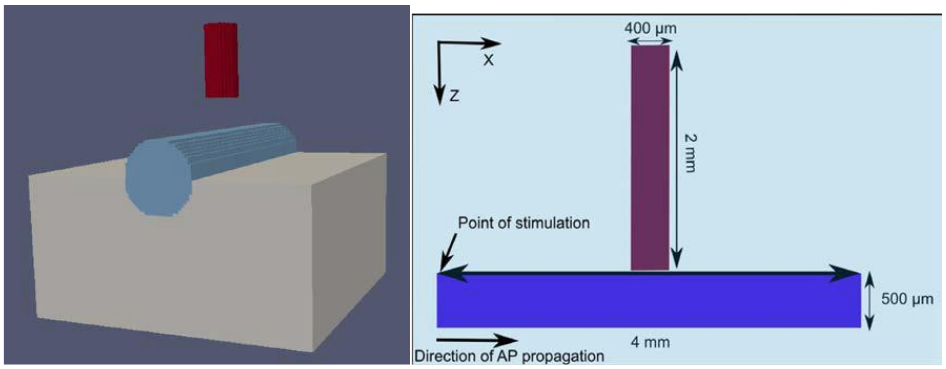

Figure 2: Nerve-fiber geometry. (Left) A neuron represented by a blue cylinder, which is half embedded in dermis tissue, and exposed to a laser fiber represented by a red vertical cylinder. (Right) Dimensions and direction of the action potential propagation are diagramed as a 2D slice.

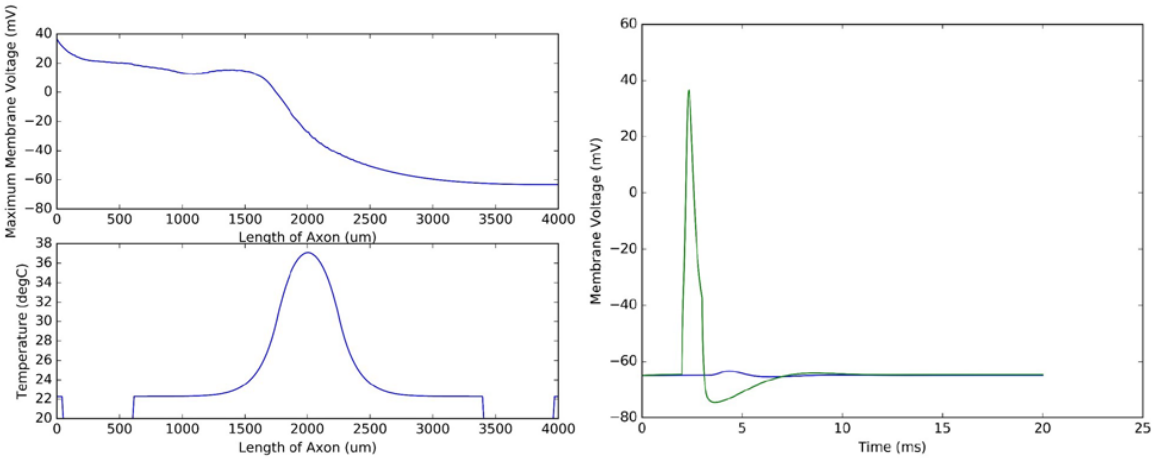

Figure 3: Modeling results for the case of a laser-induced action potential block. (Left) Temperature and maximum membrane voltage along the length of the axon. (Right) Initial stimulus and transmitted signal at other end of axon model (Green line is initial stimulus and blue is transmitted signal).

At the beginning of our LRIR tenure, the IR laser energy was simulated as a collimated top-hat beam. This is visualized in Figure 4, where the IR energy dose not exhibit refraction as it exits the optic fiber and generates a symmetric circle across the cell plate. In comparison to applied measurements, such as that obtained from a FLIR camera, we observed that the IR-induced spatial heat map is in fact asymmetric, with a tear-drop shape with the apex closest to the optical fiber. Over the duration of our LRIR tenure, we have addressed this issue by studying the relationship between the refractive

index of the core material in the fiber and air used to compute the exit (and entrance) angle of laser energy allowed. This would cause laser energy to spread out as it propagates from the fiber tip at a known angle depending on the numerical aperture of the fiber. The fiber used in the experimental work has a symmetric 12.7 degree spread of energy off the laser propagation axis calculated from its numerical aperture. This angle value was used within the Scalable Effects Simulation Environment (SESE) to more correctly model laser energy leaving the optical fiber. In Figure 4, we show the radiant flux of laser energy to visualize the path of laser energy propagation, dose of energy absorbed in the glass layer, and the resultant thermal profile at the end of the laser pulse. Because of this approach, our modeling efforts more closely represent the applied spatial heat profiles measured from the FLIR camera analysis.

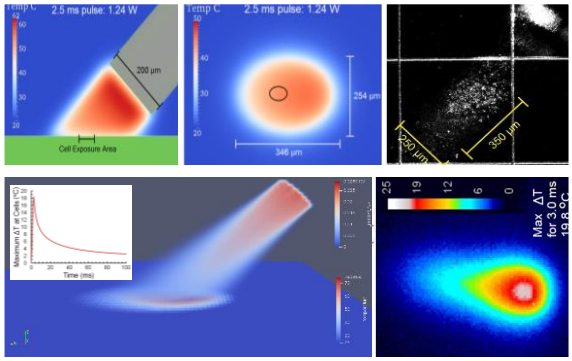

Figure 4: Advancements in IR simulations. (Top left) A collimated top-hat beam simulation of IR energy leaving the optical fiber. (Top center) Spatial distribution of IR energy at the cell surface. (Top and bottom right) FLIR camera image of the heat generated from the IR pulse. (Bottom left) IR simulation with refraction of IR energy as it exits the optical fiber.

Throughout our LRIR tenure, we have leveraged our simulation data and corroborated it with applied measurements from Opsens temperature probes to generate a detailed library of *in vitro* applied IR exposures. In Figure 5, we illustrate this by showing how an IR optical fiber placed at a 45-degree angle and 185 microns from the cell surface can generate various radiant energies (J/cm^2) and temperature changes (ΔT°C). For example, in Figure 5, we show that an IR pulse varied in width from 0.70-5.73 milliseconds

(ms) can produce between 0.13 – 1.03 J/cm^2, and a temperature change between 3.02 – 24.73 ΔT°C (data generated from SESE modeling).

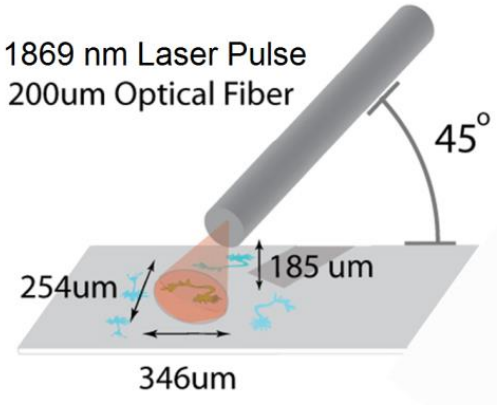

Pulse Width (ms)	Energy (mJ)	Radiant Exposure at Cells (J/cm²)	ΔT (°C)
0.70	0.86	0.13	3.02
1.37	1.68	0.25	5.91
2.15	2.64	0.39	9.28
2.73	3.35	0.49	11.78
3.58	4.39	0.64	15.45
4.10	5.03	0.74	17.70
5.01	6.14	0.90	21.62
5.47	6.71	0.98	23.61
5.73	7.03	1.03	24.73

Figure 5. Development of an in vitro platform for IR exposures. (Left) Schematic representation of critical geometries to ensure proper placement of the IR optical fiber matched simulations and applied IR measurements. (Right) Table of energy values, radiant exposures at the cells and temperature changes generated from IR pulses at different pulse widths.

Summary of Specific Aim 1: Determine the effect of IR-induced exposure on the plasma membrane

For Specific Aim 1, we utilized *in silico* IR simulations and detailed libraries of *in* vitro IR exposures as the scientific foundation to address our proposed hypothesis in this LRIR. For Aim 1, one of our pivotal findings was addressing the impact of IR exposure on membrane fluidity. From these experiments, we examined membrane fluidity in response to various IR exposures. We utilized di-4-ANEPPDHQ (di-4) dye, a fluorescent dye for which signal shift is an indicator of membrane fluidity. This polarity sensitive dye exhibits a blue shift as the membrane shifts from liquid-disordered (red) to a liquid–ordered (green) state. We calibrated the dye by measuring its fluorescent shift in response to changes in buffer temperature. This was necessary to confirm the ability of the fluorescent dye to respond to changes in membrane fluidity, and for use in future calculations. In these calibration experiments, the stage and buffer were heated to a desired temperature

and the laser was not applied. We calculated the generalized polarization value (GP) using the following equation: GP = $I_{<565} - I_{>647} / I_{<565} + I_{>647}$ (I = fluorescence intensity). As seen in Figure 6, the absolute value of the change in GP (ΔGP) becomes greater with increasing temperature, indicating an increase in membrane fluidity. A linear fit of these data were later used to estimate the temperature change of the membrane after exposure to infrared light of different pulse widths.

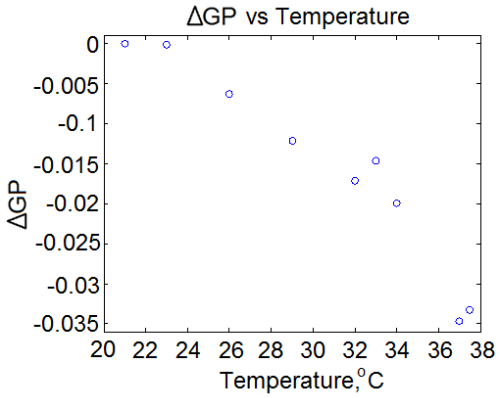

Figure 6: Change in generalized polarization for di-4-ANEPPDHQ-labeled NG108 cells as a function of ambient temperature.

Next, we exposed cells to IR energy, at 20°C. An IR pulse, with pulse width ranging from 250 μs to 3.5 ms, was delivered 0.5 sec after the start of the data acquisition. As seen from the graphs in Figure 7, the cell response is immediate, with the GP value changing instantly. Due to image cropping and pixel binning, the acquisition rate was 490 frames per second, giving a 2 ms temporal resolution. The change in the GP is shown to have a pulse width dependency, with a pulse of greater duration resulting in a more dramatic change of the GP, indicating a greater increase in the fluidity of the cell membrane. The recovery time after the exposure was very quick, with the membrane recovering sooner when exposed to a shorter pulse. The immediate response as well as the recovery times range from 100 ms to about 500 ms, suggesting that the change in the fluidity of the membrane is near instantaneous, but short-lived.

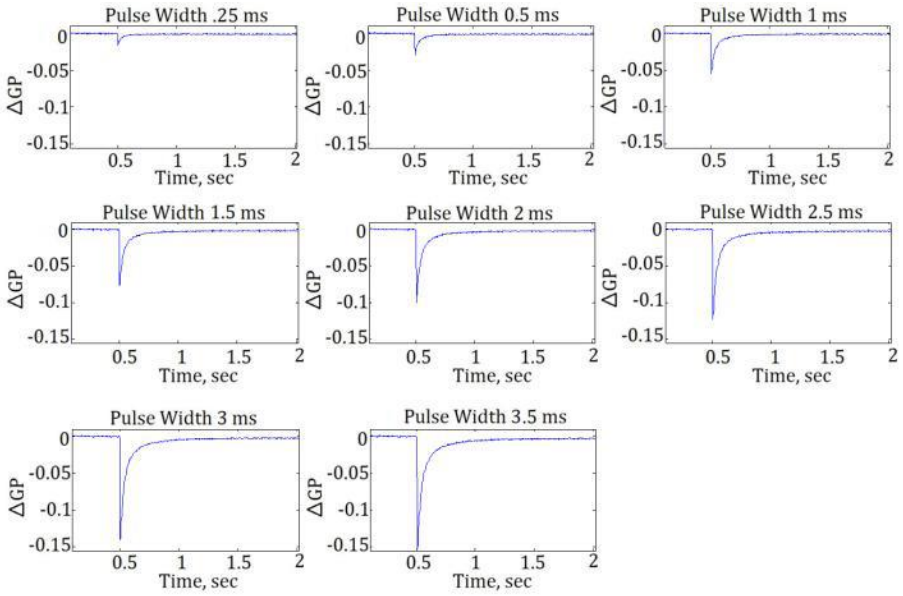

Figure 7: Membrane fluidity is modulated by an IR pulse exposure. (Top) Change in generalized polarization for di-4-ANEPPDHQ-labeled NG108 cells as a function of applied IR pulse at 20°C

At this point, we determined that IR exposure can effect membrane fluidity, but it was unclear if the extent of fluidity modulation led to membrane damage. This distinction is critical, because for infrared exposure to be a modulator of biophysical activity it must do so without long-term damage to the cell membrane. To test for this possibility, we completed second harmonic generation (SHG) imaging. This approach also utilized the polarized fluorescent reporter, di-4, but through SHG imaging the dye will only exhibit florescence with a uniformed polarity that is typically seen in the plasma membrane at steady-state. If perturbation of the membrane occurs such as poration or breakdown then there would be a non-linear polarization causing a loss of the signal. In our approach, we utilized SHG imaging against an electric field exposure that is known to cause membrane damage. As expected, we observed a loss of SHG signal upon electric field exposure. However, upon an IR pulse exposure (0.50 J/cm^2), we observed no change to SHG signal intensity throughout experiment (Figure 8). These results suggest that our particular IR exposure caused changes in membrane fluidity that did not result in membrane damage. As a result, this extended the possibility that IR exposure can modulate channel activity

within the plasma membrane. This pivotal finding provided the basis for our group to investigate intracellular dynamics that are potentially modulated by IR exposure.

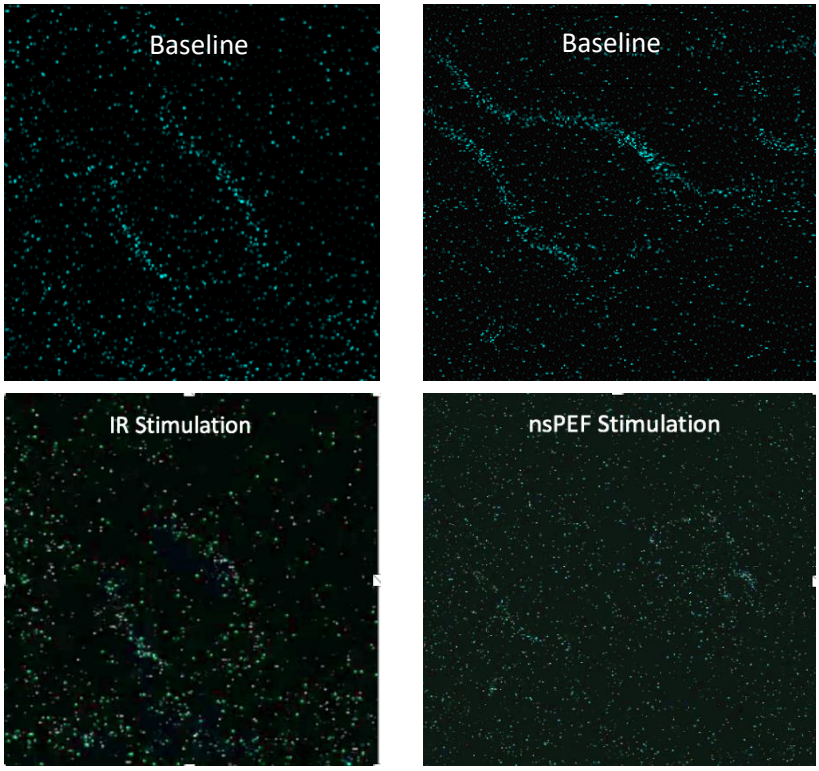

Figure 8 Second harmonic generation imaging during an IR exposure. (Left column) Images show a baseline SHG that outlines the cell membrane. Upon a 3.0 ms IR pulse, the signal remains around the membrane. (Right column) Images show a baseline SHG signal and the loss of SHG upon a nanosecond pulsed electric field (nsPEF).

Summary of Specific Aim 2: Define how calcium dynamics are modified by IR-induced FTG exposure.

During our LRIR tenure, we tested what chemical and electrical signals are modified by IR exposure. To begin, we focused on calcium ion dynamics, because the intracellular concentration of this ion often regulates the extent of second messenger activation within the cell. A pivotal finding, we uncovered was that calcium transient

amplitudes are proportional to the pulse width of the IR pulse. In Figure 9, we observed maximum calcium amplitudes from IR exposures with a 2.75 ms duration. From a 3 ms IR pulse width, we observed distinct calcium transients; however, these transients did not return to baseline. The IR energy ranged from 0.4 – 4.5 mJ for pulse widths ranging from 0.5 – 3.5 ms, respectively. Overall, these finding suggest that IR pulses can induce calcium transients in a dose-dependent manner. Furthermore, we detected a damage threshold where calcium transients are no longer able to return to baseline.

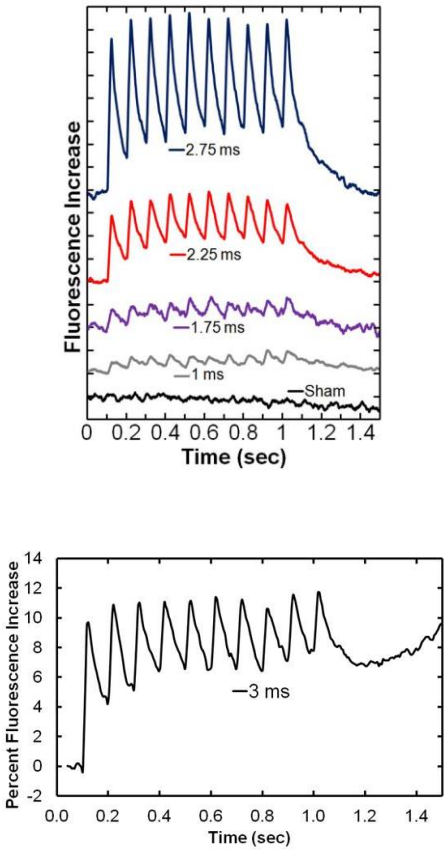

Figure 9 Calcium transients result from an IR pulse exposure. (Top) An IR exposure up to 2.75 ms can generate distinct calcium transients that return to baseline. (Bottom) A 3 ms IR exposure generates calcium transients that likely cause excitotoxicity within the cell as influx does not return to basal conditions.

In excitatory cells, an increase of intracellular calcium can lead to activation of intracellular mechanisms. Predominately, the phosphatidylinositol 4,5-bisphosphate (PIP_2) lipid signaling pathway is a key effector of calcium influx. Over our tenure, we conducted a series of experiments to investigate this lipid-signaling pathway. In Figure 10, we describe the use of a phospholipase-C (PLC) biomarker that is genetically tagged to green fluorescence protein (GFP), which upon transfection into cells can report PIP_2 activity. Specifically, under basal conditions this reporter is located along the intracellular side of the plasma membrane. Upon PIP_2 hydrolysis, the metabolites diacylglycerol (DAG) and inositol 1,4,5-trisphosphate (IP_3) are formed, and the GFP-tagged PLC reporter binds to IP_3 as it translocates to the cytosol. The translocation of GFP-tagged PLC from the membrane to the cytosol is an indicator of membrane activity that caused activation of the PIP_2 lipid-signaling pathway. We utilized this reporter by testing for potential translocation upon an IR exposure. From our experiments, we detected translocation from the membrane to the cytosol from a 5.1 mJ IR exposure. These results suggest that similar physiological activity, IR exposure can modulate second messenger signaling within excitable cells.

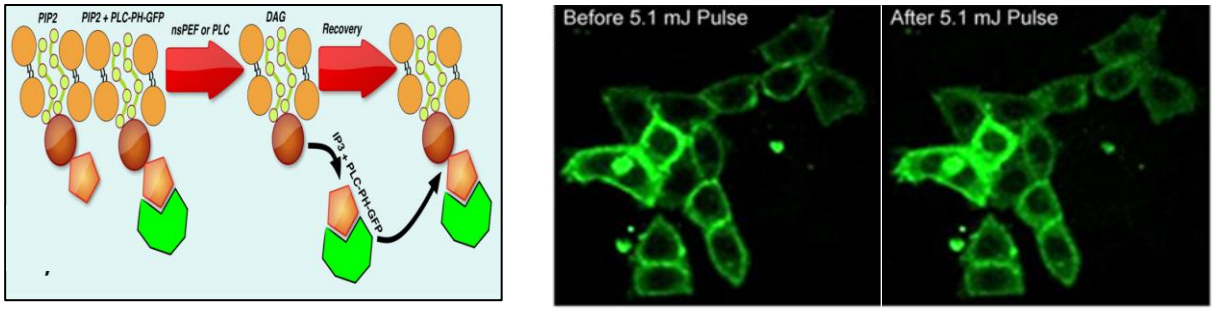

Figure 10 IR exposure causes PIP2 hydrolysis. (Left) A schematic that describes the use of the GFP-tagged PLC biomarkers as an indicator of PIP2 lipid signaling. (Right) Confocal micrographs pre- and post-IR exposure that reveal an increase in GFP present within the cytosol.

Summary of Specific Aim 3

Thus far, we have characterized how IR exposure can modify calcium dynamics in a dose-dependent manner. To expand on this effort, we tested how cell-type diversity may play a role in calcium responses from an IR exposure. This is important because the biochemical composition of a plasma membrane can vary by cell classification. For example, hippocampal neurons are involved in learning and memory where inputs are often graded and is the result of multiple synaptic inputs across different cells. NG108 cells exhibit more binary input as they function in reflex arcs in response to pain sensations (i.e. withdraw reflex from stepping on a nail). Our literature inquires revealed a broad diversity of calcium channel isoforms among both two cell types. Adding to this complexity is that calcium channel activity is unique to input specificity suggesting that the dominant calcium channel at any given time is dependent on specific input patterns.

To evaluate potential differences in calcium influx as a result of an IR exposure, we exposed primary hippocampal neurons and NG108 cells to a 3.5 ms IR pulse (4.4 mJ). We observed a robust calcium response from differentiated NG108 cells as opposed to mature hippocampal neurons. For the NG108 cells line, differentiation is the process where the cell up-regulates channels in the plasma membrane responsible for excitatory transmission. We took advantage of this process by exposing undifferentiated NG108 cells to the same IR pulse. Our observations revealed a reduced calcium response from undifferentiated NG108 cells. Overall, these series of experiments were the first to report that calcium channel diversity, even among the same cell line, can generate various calcium dynamics in response to the same IR exposure parameters.

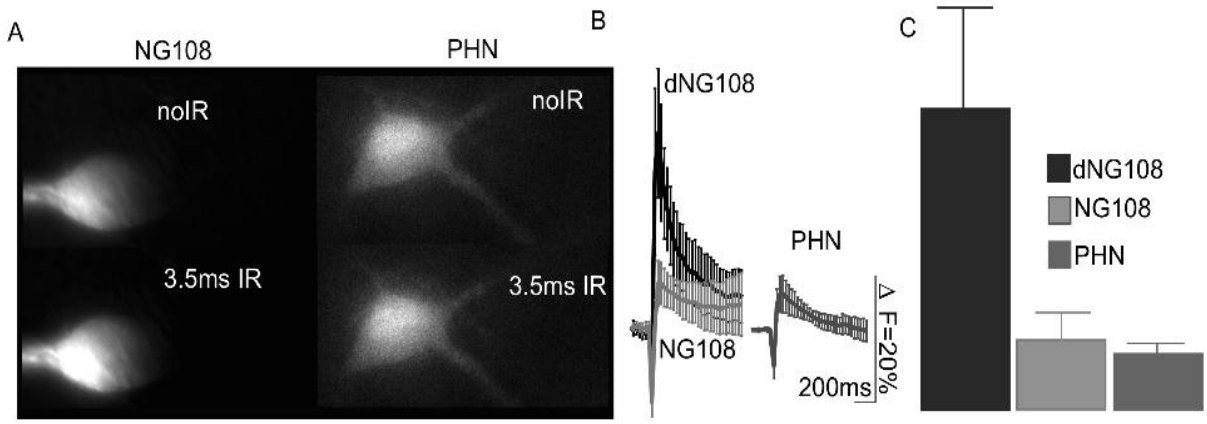

Figure 11 Calcium imaging in NG108 motor-like neurons and primary hippocampal neurons. (Left) A fluorescence indicator of calcium influx in NG 108 and primary neurons after a 3.5 ms IR pulse. (Middle) Percent change in calcium fluorescence is more robust in differentiate NG108 cells. (Right) Quantification of the peak calcium response from the different cell types

To further investigate this biophysical phenomenon, we conducted a small-molecule screen among a candidate list of calcium channels to determine which was most affected by an IR exposure. Among the candidate list was L-type calcium channels, TRPV, voltage-gated, and mechanosensitive channels. Currently, calcium antagonists offer minimal specificity when blocking unique isoforms, but are often cited to block a broad classification of channels. For example, Ruthenium red broadly inhibits TRPV channels by binding to the inner pore of the channel, which is a component present across all TRPV isoforms. Another example is GsMTx4, a peptide that selectivity inhibits cation-permeable mechanosensitive channels that are broadly detected across the TRP and Piezo channel families.

From our small molecule screen, we exposed differentiated NG-108 cells to an IR exposure, because they previously exhibited a robust calcium response to a single 3.0 ms (4.0 mJ) IR pulse. The cells were separated into two groups: control vs. exposed and the inhibitors were perfused into the cell media. Figure 12 shows the effects of each inhibitor on a calcium response from a single IR exposure. In particular, Nifedipine, Ruthenium red, and CGP-37157 did not have an effect on calcium influx. The only blocker

that revealed a change in calcium response was GsMTx4, which inhibits mechanosensitive channels. This result is very interesting for our future efforts, because it suggests that IR exposure can modulate the mechanical properties of channels at the plasma membrane. Furthermore, our results from Aim 1 corroborate this finding as we detected an increase membrane fluidity from an IR pulse, which is a key initiator of mechanosensitive biophysical mechanisms in excitable cells.

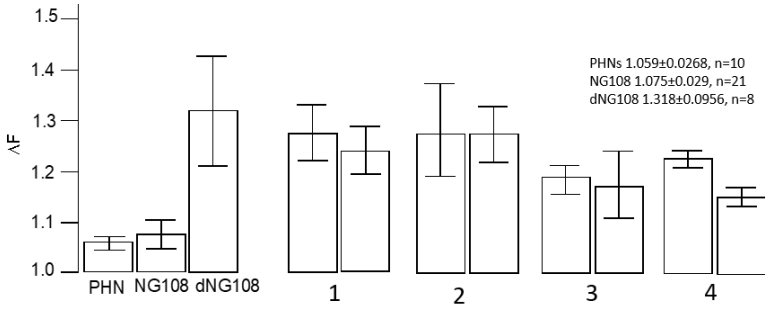

1. Nifedipine
Before 1.29±0.058, n=5
After 1.25±0.05, n=5

2. Ruthenium red
Before 1.29±0.11 n=5
After 1.29=0.058 n=5

3. CGP-37157
Before 1.2±0.03 n=4
After 1.18±0.08 n=4

4. GsMTx4
Before 0.24±0.0178 n=4
After 0.16±0.022 n=4

Figure 12 Quantification of fluorescence calcium response across primary hippocampal neurons (PHN) and undifferentiated or differentiated (d) NG108 cells. We selected dNG 108 cells for the inhibitor drug screen. The use of GsMTx4, a peptide antagonist, was the only inhibitor to impact calcium transients induce by a single 3.0 ms IR pulse.

Overall, from our LRIR tenure, we examined the biophysical effects of a single IR pulse exposure to excitable cells, from which we would measure membrane permeability, second messenger activity, or calcium dynamics. From these specific aims, we were not only able to elucidate channels that play a role in IR-mediated bioeffects, but also the electrophysical impact of the pulse. For example, if the single IR pulse was delivered upon a current injection to a neuron, then we would observe an action potential block. On the contrary, if an IR pulse was delivered without a simultaneous current injection, then we

would detect an action potential response in NG-108 cells, and a graded potential in primary hippocampal neurons.

For the future direction of our efforts, we decided to leverage our experimental findings, and advance the IR exposure design. To this end, we set forth to develop IR exposure parameters that more closely represented neurophysiological signaling from a synaptic connection. For example, upon basal conditions, neurons will exhibit spontaneous firing. Typically, these membrane potentials exhibit a 2 Hz repetition rate, which is altered upon high or low intensity stimulation. Working within this paradigm, we generated an IR pulse at a similar rate seen with synaptic transmission. By recording temperature changes with an Opsens probe that was placed next to the IR optical fiber, we were able to scan various input parameters to match the frequency seen from synaptic transmission. As a result, we generated IR pulses with different repetition frequencies. For example, we designed a sub-microsecond pulse at a 2Hz repetition frequency. This IR delivery exhibited pulses with a ΔT of 14°C at 2 Hz (Figure 13). Furthermore, the firing pattern matched the firing rate of spontaneous activity from somatic recording. Through our investigations, we also observed that higher frequencies would generate temperature transients that, unlike a 2 Hz repetition rate, would not return to baseline. Instead, the 5 Hz stimulations represented an additivity of thermal gradients that generated a "continuous wave" profile that averaged a ΔT of 3°C for the IR pulse train

Figure 13 IR pulse frequencies. (Left and Center) IR pulse repetition rates at 1-2 Hz deliver distinct temperature transients. (Right) IR pulses at 5 Hz display an additivity of thermal gradients.

We next investigated the potential bioeffects due to these advanced IR exposure parameters. In doing so, we tested their impact on action potential propagation that was induced by a square wave current injection. From the 2 Hz repetition rate, we observed irregular firing patterns, and a loss of action potentials. Interestingly, the 5 Hz repetition rate caused a complete block of action potential propagation that was reversible upon termination of the IR pulse train. These results suggest that IR pulses with frequencies similar to spontaneous neuronal activity have a significant impact on neuronal electrical properties. The extent to which the cell remains healthy and potential long-term effects are still unknown and is the focus of our future efforts. On the other hand, IR pulses that exhibit a “continuous” heat block can inhibit action potential propagation, but effects are immediately reversible. Overall, the impact of these advanced IR pulse frequencies are the focus of future efforts upon completion of this LRIR. Our future goal is to understand how IR pulse delivery that mimics physiological signaling can impact neuronal communication.

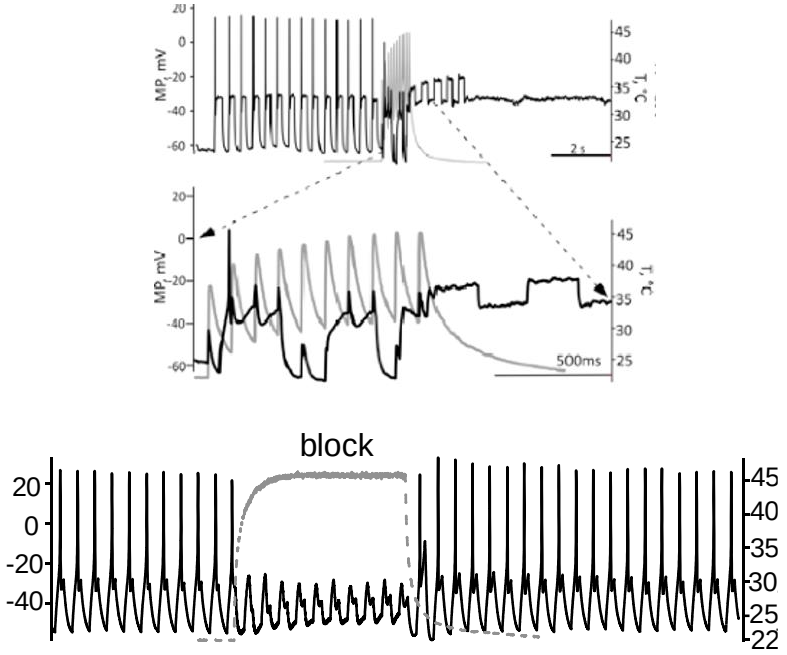

Figure 14 Bioeffects of IR pulse frequency exposure. (Top) Delivery of a 2 Hz sub-microsecond IR pulse resulted in a loss of action potential propagation. (Bottom) Delivery of a 5 Hz IR pulse train resulted in transient blocking of action potentials that reversed after the IR exposure.

Conclusions and Future Directions

The effort given to this LRIR tenure has resulted in numerous publications, proceedings, presentations, and technical reports. The AFOSR LRIR platform has allowed us to collaborate with academic institutions (i.e. Vanderbilt Biophotonics center) to produce innovative basic research to evaluate the biophysical interactions related to IR exposure. Our future efforts will further investigate the bioeffects generated from repetitive IR exposures and compare and contrast these effects to the published literature. We aim to collaborate with fellow AFRL scientists to generate an *ex vivo* experimental design for IR exposure applications. This will allow us to have a deeper understanding of how IR exposure can play a role within an *in vivo* environment.

Funding Summary by Cost Category—Be Specific (by FY, $K):

	In House	Capital Equip. >$5K each	On-Site Contractor	Misc. Supplies	Total
FY18		5	140	5	150
FY19		5	140	5	150
FY20		5	140	5	150

Appendix A: In-house Activities

Personnel	Degree	Discipline	Involvement
Christopher Valdez (AFRL)	Ph.D.	Neuroscience	50%
Chad Oian (AFRL)	MSc.	Computer Science	20%
Anna Sedelnikova	MSc.	Neuroscience	100%
Ronald Barnes Jr.	Ph.D.	Electrical Engineering	10%
Bennett L. Ibey	Ph.D.	Biomedical Engineering	10%

Patent Disclosure:

1. Walsh AJ, Beier HT., Ibey BL., “Neuron inhibition by infrared light” US Patent App.2018/ 0224423
2. Beier, Hope T., Bennett Ibey, and Caleb C. Roth. "Biological cell and tissue fixation by laser irradiation.” U.S. Patent Application No. 14/670,067.

Publications:

1. Sedelnikova, Anna et al., (2020) “An evaluation of the effects of different thermal gradient profiles (produced by pulsed infrared laser) on neuronal excitability modulation,” In preparation for Journal of Neuroengineering
2. Sedelnikova, Anna et. al., (2019) “Dissecting the diversity of excitatory and inhibitory responses to a single short infrared laser pulse in postnatal hippocampal neurons and motor neuron-like differentiated NG108 cells.” *In Submission to Stinfo for Journal of Neuroengineering*
3. Tolstykh, Gleb P., et al., (2017) "Ryanodine and IP 3 receptor-mediated calcium signaling play a pivotal role in neurological infrared laser modulation." Neurophotonics 4.2: 025001
4. Walsh, A. J., et al., (2017). Short infrared laser pulses block action potentials in neurons. In *Optogenetics and Optical Manipulation* (Vol. 10052, p. 100520J). International Society for Optics and Photonics.

Proceedings:

1. Tolstykh, Gleb P., et al. "Infrared laser-induced fast thermal gradient affects the excitability of primary hippocampal neurons." Optical Interactions with Tissue and Cells XXXI. Vol. 11238. International Society for Optics and Photonics, 2020.
2. Tolstykh, Gleb P., et al. "Pulsed infrared laser activates intracellular signaling in NG108 cells." Optical Interactions with Tissue and Cells XXXI. Vol. 11238. International Society for Optics and Photonics, 2020.
3. Valdez, Christopher. Biophysics of Neuromodulation by Rapid Deposition of Energy Annual Report. 711 HPW/RHDR JBSA Fort Sam Houston United States, 2019.
4. Beier, H. T., & Ibey, B. L. (2019, April). Optical Interactions with Tissue and Cells XXX. In Proc. of SPIE Vol (Vol. 10876, pp. 1087601-1).
5. Walsh, Alex J., et al. "Fluorescence lifetime imaging of calcium flux in neurons in response to pulsed infrared light." Multiphoton Microscopy in the Biomedical Sciences XVII. Vol. 10069. International Society for Optics and Photonics, 2017.
6. Walsh, Alex J., et al. "Short infrared laser pulses increase cell membrane fluidity." SPIE. Vol. 10062. 2017.
7. Walsh, Alex J., et al. "Short infrared laser pulses block action potentials in neurons." Optogenetics and Optical Manipulation. Vol. 10052. International Society for Optics and Photonics, 2017.
8. Moen, Erick K., et al. "The role of membrane dynamics in electrical and infrared neural stimulation." SPIE. Vol. 9719. 2016.
9. Roth, Caleb C., et al. "Short infrared (IR) laser pulses can induce nanoporation." Clinical and Translational Neurophotonics; Neural Imaging and Sensing; and Optogenetics and Optical Manipulation. Vol. 9690. International Society for Optics and Photonics, 2016
10. Translational Neurophotonics; Neural Imaging and Sensing; and Optogenetics and Optical Manipulation. Vol. 9690. International Society for Optics and Photonics, 2016.Olsovsky, Cory A., et al. "Origins of intracellular calcium mobilization evoked by infrared laser stimulation." Optical Interactions with Tissue and Cells XXVI. Vol. 9321. International Society for Optics and Photonics, 2015.

Invited Lectures, Presentations, Talks, etc:

1. Valdez, C.M., “The role of infrared exposure on neuronal connectivity” Vanderbilt University 2019
2. Valdez, C.M., “How does infrared exposure impact neuronal connectivity,” UT-San Antonio, 2019

Professional Activities:

1. BiOS/Photonics West, 2020 Optical Interaction with Tissue and Cells XXVII Conference
2. Society for Neuroscience, 2019

Honors Received:

1. 711 Human Performance Wing- Category III Civilian of the quarter, 2019